# Field emission from graphene based composite thin films

Goki Eda,[1,a)] H. Emrah Unalan,[2] Nalin Rupesinghe,[2] Gehan A. J. Amaratunga,[2] and Manish Chhowalla[1,b)]
[1]*Department of Materials Science and Engineering, Rutgers University, Piscataway, New Jersey 08854, USA*
[2]*Electrical Engineering Division, Department of Engineering, University of Cambridge, 9 J J Thomson Avenue, Cambridge CB3 0FA, United Kingdom*

(Received 17 September 2008; accepted 24 October 2008; published online 9 December 2008)

Field emission from graphene is challenging because the existing deposition methods lead to sheets that lay flat on the substrate surface, which limits the field enhancement. Here we describe a simple and general solution based method for the deposition of field emitting graphene/polymer composite thin films. The graphene sheets are oriented at some angles with respect to the substrate surface leading to field emission at low threshold fields ($\sim 4$ V $\mu m^{-1}$). Our method provides a route for the deposition of graphene based thin film field emitter on different substrates, opening up avenues for a variety of applications. © *2008 American Institute of Physics*. [DOI: 10.1063/1.3028339]

The intriguing properties of graphene arising from its unique energy-momentum dispersion relation have given rise to numerous fundamental studies.[1] Promising applications range from composites,[2–4] sensors,[5,6] spintronic devices,[7,8] nonvolatile memory[9] to transparent and conducting electrodes in organic solar cells, light emitting diodes, and liquid crystal displays.[10–13]

Although there has been tremendous interest in cold cathode field emission from carbon materials ranging from diamond,[14,15] amorphous carbon,[16] vertically aligned multi[17–19] and single walled carbon nanotubes,[20] and carbon nanosheets,[21–23] electron emission from graphene has yet to be reported. Field emission from composites based on graphite flakes dispersed in insulating medium has been investigated.[24,25] Electron emission in composites occurs via field enhancement from graphitic protrusions. The geometrical features of graphene should increase field enhancement, allowing the extraction of electrons at lower threshold electric fields.[26] The electric field enhancement factor ($\beta$) for laterally macroscopic but atomically thin graphene may be of the order of a few thousand. To take advantage of the high field enhancement, graphene sheets would have to stand on their edges and not lay laterally flat on the substrate. Vertically oriented carbon nanosheets consisting of several layers with good field emission properties grown at high temperature have been reported.[21–23] Virtually all deposition methods reported thus far for graphene yield sheets laying flat on the substrate. Here we report field emission from randomly but nonlaterally oriented graphene in polymer host deposited using a simple solution based deposition method. Our approach utilizes the scheme of composite preparation[2] to realize the concept of field emitting composite film[24] in which graphene sheets represent the field emission sites. Field emission is demonstrated to occur at low threshold fields ($\sim 4$ V/$\mu$m) comparable to those of typical carbon nanotube arrays[19] and analogous composite materials based on carbon nanotubes.[27] The field enhancement factor in the emitting samples was extracted to be $\sim 1200$, assuming a work function of 5 eV.

The most common method for obtaining individual graphene sheets is cleaving of graphite ("Scotch tape method").[28] An alternative route to graphene is reduction of graphene oxide (GO),[29–31] which can be readily produced in large quantities in aqueous suspensions.[32] Processability of GO enable incorporation into polymer[2] and ceramic[3] matrices where individual graphene sheets remain dispersed. The pioneering work in graphene based polymer composites[2,33] was realized by the ability to obtain chemically functionalized GO which could be suspended in organic solvents with common polymers such as polystyrene. We utilized the graphene-polystyrene composites methodology to deposit thin films by spin coating to achieve nonlaterally oriented graphene sheets.

Graphite oxide prepared using modified Hummers method[34] was chemically functionalized by phenyl isocyanate (see Ref. 33 for detailed methodology) and dissolved in dimethylformamide at a concentration of 1 mg/mL. A homogenous stable suspension of submicron sized functionalized GO sheets was achieved by ultrasonicating the suspension for 10 h. An appropriate amount of linear monodisperse polystyrene ($M_w$=2 014 000 g/mol, polydispersity index =1.04, Scientific Polymer Products) was dissolved in the suspension to achieve a graphene-to-polystyrene volume fraction of 10%. Chemical reduction of phenyl isocyanate-treated functionalized GO was achieved by adding 0.1 ml of dimethylhydrazine into 5 ml suspension and heating the mixture to 80 °C for 24 h. The suspension was spin coated onto degenerately doped silicon (0.002–0.005 Ω cm) in a glovebox. After deposition, the composite thin film was annealed at 200 °C for 10 h to remove residual solvents and also to achieve further reduction of GO.

The orientation of the graphene sheets in the composite thin films (thickness=10–50 nm) can be varied from randomly oriented to laterally oriented by controlling the spin coating speeds. The atomic force microscope (AFM) images and corresponding line scans of the composite thin films deposited at two shear rates are shown in Figs. 1(a)–1(d). The graphene sheets are readily visible in the figures as submicron sized flakes. At low spin coating speeds, graphene sheets are densely distributed over the substrate [Fig. 1(a)]. The brighter regions in the AFM image in Fig. 1(a) represent graphene flakes protruding above the surface, as indicated

a)Electronic mail: goki@eden.rutgers.edu.
b)Author to whom correspondence should be addressed. Electronic mail: goki@manish1@rci.rutgers.edu.

 

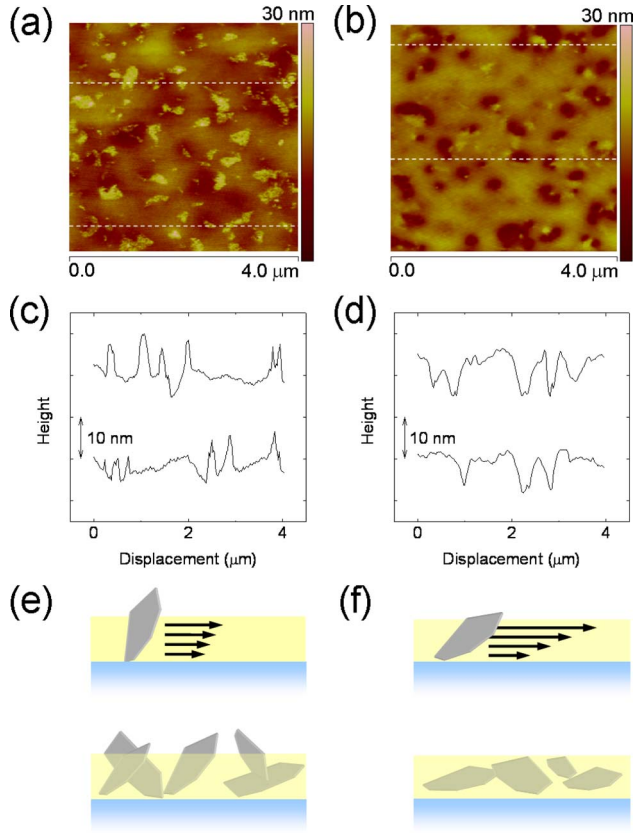


FIG. 1. (Color online) AFM images (Digital Instruments, Nanoscope IV, tapping mode, force constant=40 N/m, tip curvature=10 nm) and corresponding line scans of [(a) and (c)] 600 rpm and [(b) and (d)] 2000 rpm thin films. Brighter regions readily visible in image (a) represent graphene sheets protruding from the film surface. Schematic of the spin coating process for the (e) low and (f) high spin coating speeds.

schematically in Fig. 1(e). From AFM profilometry, the protrusions typically appear as 5–10 nm peaks above the film surface [Fig. 1(b)]. At higher spin coating speeds, the sheets are sparsely distributed [Fig. 1(b)] and oriented almost parallel to the substrate surface and often embedded within the polystyrene [Fig. 1(d)]. At low spin coating speeds, the shear force is sufficiently small to maintain the random orientation of graphene sheets and the polymer solidifies before the sheets align parallel to the substrate surface, as schematically described in [Figs. 1(e) and 1(f)].

In order for field emission to occur, electrons must be injected from the back contact into the film and then emitted into vacuum. Therefore, efficient conduction through the film and large field enhancement in proximity of the film surface are essential for electron emission. GO is insulating but can be reduced to disorder-containing graphene in polystyrene to render the composite thin films conductive.[3] The through film resistance was found to be very low but accurate measurements were challenging due to the film thinness. Therefore, we used lateral resistivity to infer the orientation of the graphene sheets. The lateral resistivities were found to be higher for films deposited at low and high spin coating speeds (Fig. 2). Changes in lateral resistivity with spin coating speed can be explained by the two following effects: changes in the orientation at low spin coating speeds and decreased percolation of graphene sheets at high spin speeds. That is, as the spin coating speed is increased, graphene sheets become more preferentially oriented parallel to the substrate, thus facilitating in-plane electrical conduction.

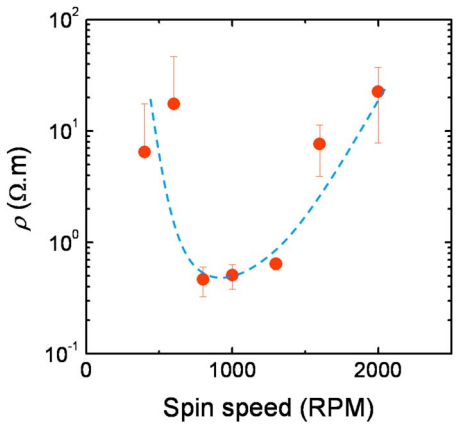


FIG. 2. (Color online) The lateral resistivity of the graphene/polystyrene composite thin films vs the spin coating speeds. Gold was thermally evaporated onto the composite films deposited on glass substrates and used as the electrodes. The lateral resistivity $\rho$ was calculated assuming $\rho=R_s t$ where $R_s$ is the sheet resistance and $t$ is the film thickness.

However, at very high spin coating speeds, the distance between graphene sheets increases to the point where percolation among the sheets is diminished, which decreases the conductivity.

Field emission of the composite thin films was measured as a function of the spin coating speeds. In order to confirm that the measured field emission characteristics were due to graphene and not artifacts, measurements of the bare substrate and pure polystyrene were also performed and revealed no emission. The current density versus the applied field for two films deposited at 600 and 2000 rpm are shown in Fig. 3. It can be seen from the figure that the threshold field required to drive a current of $10^{-8}$ A/cm$^2$ is significantly lower for the 600 rpm sample (~4 V/$\mu$m) compared to the 2000 rpm sample (~11 V/$\mu$m). The much lower threshold field for electron emission in the 600 rpm sample suggests significantly higher field enhancement factor. Furthermore, the current from the 2000 rpm sample does not saturate at high fields, suggesting that the emission is limited by the resistance of the thin film. The low threshold field emission and higher current with increasing field further support the AFM and electrical measurement data. The 4 V/$\mu$m threshold field for the graphene comosite samples is higher than the lowest threshold fields of carbon nanotubes[35] and other carbon-based materials[15,36] (0.5–1 V/$\mu$m) reported in the literature. However, such low threshold fields in carbonaceous materials have been found to be a consequence of local inhomogeneities (i.e., large protrusion) and careful

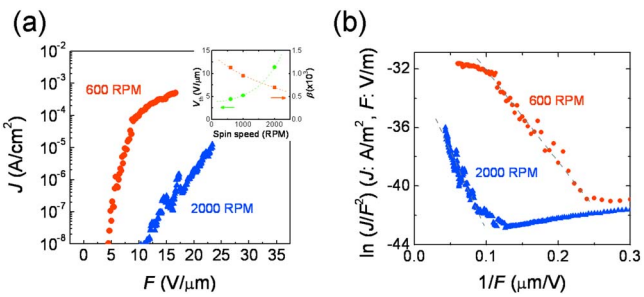


FIG. 3. (Color online) The (a) field emission current density vs applied field for graphene/polystyrene composite thin films deposited at 600 and 2000 rpm. (b) The corresponding FN plots. The inset shows the trend of the threshold voltage and field enhancement factor as a function of the spin coating speeds.

analysis reveals that for uniformly spaced emitters, field emission occurs at several $V/\mu m$.[19] The maximum current density we obtained was 1 $mA/cm^2$, which is below the highest value reported for carbon nanotubes ($\sim 4$ $A/cm^2$) (Ref. 37) but consistent with vertically aligned nanotubes when space charge within the emitted beam is not mediated.[38]

The field enhancement factor ($\beta$) can be extracted from the field emission data, assuming that the data in Fig. 3(a) are described by the Fowler–Nordheim (FN) equation.[39] $\beta$ can be obtained from the linear region of the FN plot shown in Fig. 3(b) and assuming the work function of graphene to be 5 eV. The curvature of FN plot at low field may be attributed to the statistical variation of geometrical, structural, and electronic characteristics of field emitting sites.[40] The $\beta$ values from the FN plots were found to be $\sim 1200$ and 700 for the 600 and 2000 rpm samples, respectively. We also found that presence of polystyrene is necessary to achieve large field enhancement by comparing field emission from polystyrene free thin films. Thus, it appears that for composite films deposited at 600 rpm, field enhancement is facilitated by the polystyrene matrix,[27] which enables the graphene sheets to be oriented at some angle with respect to the substrate surface. Besides the morphological and topographical factors mentioned above, field enhancement can also be determined by interfacial effects. Graphene sheets are likely to be covered by polystyrene forming metal-insulator-vacuum interface[25] or partially exposed forming a triple junction,[41] which complicates the physical mechanism of field emission.[42,43] Image analysis of the samples after the field emission measurements revealed that the surface was largely unchanged, indicating that cold cathode emission is responsible for the observed data and is not due to artifacts such as microarcing.

A simple method to deposit graphene cold cathodes for field emission has been demonstrated. By dispersing the graphene in polystyrene and depositing the composite such that the sheets are somewhat vertically aligned leads to an increase in the field enhancement factor as high as 1200. This allows electron emission to occur at low threshold voltage, making graphene an excellent candidate for field emission applications. The ability to deposit field emitting graphene composite thin films from solution could allow large area deposition on inexpensive and flexible substrates which may open up exciting applications.

This work was funded by the National Science Foundation CAREER Award (ECS 0543867).

[1] A. K. Geim and K. S. Novoselov, Nature Mater. **6**, 183 (2007).
[2] S. Stankovich, D. A. Dikin, G. H. B. Dommett, K. M. Kohlhaas, E. J. Zimney, E. A. Stach, R. D. Piner, S. T. Nguyen, and R. S. Ruoff, Nature (London) **442**, 282 (2006).
[3] S. Watcharotone, D. A. Dikin, S. Stankovich, R. Piner, I. Jung, G. H. B. Dommett, G. Evmenenko, S. E. Wu, S. F. Chen, C. P. Liu, S. T. Nguyen, and R. S. Ruoff, Nano Lett. **7**, 1888 (2007).
[4] T. Ramanathan, A. A. Abdala, S. Stankovich, D. A. Dikin, M. Herrera-Alonso, R. D. Piner, D. H. Adamson, H. C. Schniepp, X. Chen, R. S. Ruoff, S. T. Nguyen, I. A. Aksay, R. K. Prud'Homme, and L. C. Brinson, Nat. Nanotechnol. **3**, 327 (2008).
[5] F. Schedin, A. K. Geim, S. V. Morozov, E. W. Hill, P. Blake, M. I. Katsnelson, and K. S. Novoselov, Nature Mater. **6**, 652 (2007).
[6] I. I. Barbolina, K. S. Novoselov, S. V. Morozov, S. V. Dubonos, M. Missous, A. O. Volkov, D. A. Christian, I. V. Grigorieva, and A. K. Geim, Appl. Phys. Lett. **88**, 013901 (2006).
[7] E. W. Hill, A. K. Geim, K. Novoselov, F. Schedin, and P. Blake, IEEE Trans. Magn. **42**, 2694 (2006).
[8] N. Tombros, C. Jozsa, M. Popinciuc, H. T. Jonkman, and B. J. van Wees, Nature (London) **448**, 571 (2007).
[9] T. J. Echtermeyer, M. C. Lemme, M. Baus, B. N. Szafranek, A. K. Geim, and H. Kurz, IEEE Electron Device Lett. **29**, 952 (2008).
[10] G. Eda, G. Fanchini, and M. Chhowalla, Nat. Nanotechnol. **3**, 270 (2008).
[11] X. Wang, L. Zhi, and K. Mullen, Nano Lett. **8**, 323 (2007).
[12] P. Blake, P. D. Brimicombe, R. R. Nair, T. J. Booth, D. Jiang, F. Schedin, L. A. Ponomarenko, S. V. Morozov, H. F. Gleeson, E. W. Hill, A. K. Geim, and K. S. Novoselov, Nano Lett. **8**, 1704 (2008).
[13] H. A. Becerill, J. Mao, Z. Liu, R. M. Stoltenberg, Z. Bao, and Y. Chen, ACS Nano **2**, 463 (2008).
[14] C. Wang, A. Garcia, D. C. Ingram, M. Lake, and M. E. Kordesche, Electron. Lett. **27**, 1459 (1991).
[15] K. Okano, S. Koizumi, S. R. P. Silva, and G. A. J. Amaratunga, Nature (London) **381**, 140 (1996).
[16] G. A. J. Amaratunga and S. R. P. Silva, Appl. Phys. Lett. **68**, 2529 (1996).
[17] W. A. De Heer, A. Chatelain, and D. Ugarte, Science **270**, 1179 (1995).
[18] A. G. Rinzler, J. H. Hafner, P. Nikolaev, P. Nordlander, D. T. Colbert, R. E. Smalley, L. Lou, S. G. Kim, and D. Tomanek, Science **269**, 1550 (1995).
[19] K. B. K. Teo, M. Chhowalla, G. A. J. Amaratunga, W. I. Milne, G. Pirio, P. Legagneux, F. Wyczisk, D. Pribat, and D. G. Hasko, Appl. Phys. Lett. **80**, 2011 (2002).
[20] Y. Saito, K. Hamaguchi, T. Nishino, K. Hata, K. Tohji, A. Kasuya, and Y. Nishina, Jpn. J. Appl. Phys., Part 2 **36**, L1340 (1997).
[21] S. G. Wang, J. J. Wang, P. Miraldo, M. Y. Zhu, R. Outlaw, K. Hou, X. Zhao, B. C. Holloway, D. Manos, T. Tyler, O. Shenderova, M. Ray, J. Dalton, and G. McGuire, Appl. Phys. Lett. **89**, 183103 (2006).
[22] K. Hou, R. A. Outlaw, S. Wang, M. Zhu, R. A. Quinlan, D. M. Manos, M. E. Kordesch, U. Arp, and B. C. Holloway, Appl. Phys. Lett. **92**, 133112 (2008).
[23] J. Wang and T. Ito, Diamond Relat. Mater. **16**, 589 (2007).
[24] S. Bajic and R. V. Latham, J. Phys. D: Appl. Phys. **21**, 200 (1988).
[25] A. P. Burden, H. E. Bishop, M. Brierley, J. M. Friday, C. Hood, P. G. A. Jones, A. Y. Kyazov, W. Lee, R. J. Riggs, V. L. Shaw, and R. A. Tuck, J. Vac. Sci. Technol. B **18**, 900 (2000).
[26] S. Watcharotone, R. S. Ruoff, and F. H. Read, Phys Procedia **1**, 71 (2008).
[27] P. C. P. Watts, S. M. Lyth, E. Mendoza, and S. R. P. Silva, Appl. Phys. Lett. **89**, 103113 (2006).
[28] K. S. Novoselov, A. K. Geim, S. V. Morozov, D. Jiang, Y. Zhang, S. V. Dubonos, I. V. Grigorieva, and A. A. Firsov, Science **306**, 666 (2004).
[29] R. S. Ruoff, Nat. Nanotechnol. **3**, 10 (2008).
[30] S. Gijie, S. Han, M. Wang, K. L. Wang, and R. B. Kaner, Nano Lett. **7**, 3394 (2007).
[31] C. Gomez-Navarro, T. R. Weitz, A. M. Bittner, M. Scolari, A. Mews, M. Burghard, and K. Kern, Nano Lett. **7**, 3499 (2007).
[32] S. Stankovich, R. D. Piner, X. Q. Chen, N. Q. Wu, S. T. Nguyen, and R. S. Ruoff, J. Mater. Chem. **16**, 155 (2006).
[33] S. Stankovich, R. Piner, S. T. Nguyen, and R. S. Ruoff, Carbon **44**, 3342 (2006).
[34] M. Hirata, T. Gotou, S. Horiuchi, M. Fujiwara, and M. Ohba, Carbon **42**, 2929 (2004).
[35] Q. H. Wang, T. D. Corrigan, J. Y. Dai, R. P. H. Chang, and A. R. Krauss, Appl. Phys. Lett. **70**, 3308 (1997).
[36] I. Musa, D. A. I. Munindrasdasa, G. A. J. Amaratunga, and W. Eccleston, Nature (London) **395**, 362 (1998).
[37] W. Zhua, C. Bower, O. Zhou, G. Kochanski, and S. Jin, Appl. Phys. Lett. **75**, 873 (1999).
[38] N. L. Rupesinghe, M. Chhowalla, K. B. K. Teo, and G. A. J. Amaratunga, J. Vac. Sci. Technol. B **21**, 338 (2003).
[39] R. H. Fowler and L. Nordheim, Proc. R. Soc. London, Ser. A **119**, 173 (1928).
[40] J. D. Levine, J. Vac. Sci. Technol. B **13**, 553 (1995).
[41] I. Alexandrou, E. Kymakis, and G. A. J. Amaratunga, Appl. Phys. Lett. **80**, 1435 (2002).
[42] K. H. Bayliss and R. V. Latham, Proc. R. Soc. London, Ser. A **403**, 285 (1986).
[43] R. G. Forbes, Solid State Commun. **45**, 779 (2001).